J|A|C|S ARTICLES

Published on Web 10/29/2009

Superbasicity of a Bis-guanidino Compound with a Flexible Linker: A Theoretical and Experimental Study

Martyn P. Coles,*,† Pedro J. Aragón-Sáez,† Sarah H. Oakley,† Peter B. Hitchcock,† Matthew G. Davidson,‡ Zvonimir B. Maksić,§ Robert Vianello,§ Ivo Leito,|| Ivari Kaljurand,|| and David C. Apperley⊥

Department of Chemistry, University of Sussex, Falmer, Brighton BN1 9QJ, U.K., Department of Chemistry, University of Bath, Bath BA2 7AY, U.K., Quantum Organic Chemistry Group, Division of Organic Chemistry and Biochemistry, Rudjer Bošković Institute, P.O. Box 180, HR-10 002 Zagreb, Croatia, Institute of Chemistry, University of Tartu, Ravila 14a, 50411 Tartu, Estonia, and Department of Chemistry, University Science Laboratories, University of Durham, South Road, Durham DH1 3LE, U.K.

Received August 5, 2009; E-mail: m.p.coles@sussex.ac.uk

Abstract: The bis-guanidino compound $H_2C\{hpp\}_2$ (**I**; hppH = 1,3,4,6,7,8-hexahydro-2*H*-pyrimido[1,2-*a*]pyrimidine) has been converted to the monocation [**I**-H]$^+$ and isolated as the chloride and tetraphenylborate salts. Solution-state spectroscopic data do not differentiate the protonated guanidinium from the neutral guanidino group but suggest intramolecular "—N—H···N=" hydrogen bonding to form an eight-membered C_3N_4H heterocycle. Solid-state CPMAS ^{15}N NMR spectroscopy confirms protonation at one of the imine nitrogens, although line broadening is consistent with solid-state proton transfer between guanidine functionalities. X-ray diffraction data have been recorded over the temperature range 50−273 K. Examination of the carbon−nitrogen bond lengths suggests a degree of "partial protonation" of the neutral guanidino group at higher temperatures, with greater localization of the proton at one nitrogen position as the temperature is lowered. Difference electron density maps generated from high-resolution X-ray diffraction studies at 110 K give the first direct experimental evidence for proton transfer in a poly(guanidino) system. Computational analysis of **I** and its conjugate acid [**I**-H]$^+$ indicate strong cationic resonance stabilization of the guanidinium group, with the nonprotonated group also stabilized, albeit to a lesser extent. The maximum barrier to proton transfer calculated using the Boese−Martin for kinetics method was 2.8 kcal mol^{-1}, with hydrogen-bond compression evident in the transition state; addition of zero-point vibrational energy values leads to the conclusion that the proton transfer is barrierless, implying that the proton shuttles freely between the two nitrogen atoms. Calculations determining the gas-phase proton affinity and the pK_a in acetonitrile both indicate that compound **I** should behave as a superbase. This has been confirmed by spectrophotometric titrations in MeCN using polyphosphazene references, which give an average pK_a of 28.98 ± 0.05. Triadic analysis indicates that the dominant term causing the high basicity is the relaxation energy.

Introduction

Substituted guanidines in which one or more groups replace the hydrogens of $HN{=}C(NH_2)_2$ retain the strongly basic characteristics of the parent compound and function through protonation of the imine nitrogen to form the corresponding guanidinium cation. The strength of the basicity is governed by a number of factors that correlate to the ease with which the resultant positive charge is delocalized throughout the "CN_3" core of the molecule.[1] A simple strategy to generate "superbases" (defined as a compound with a pK_a greater than that of the proton sponge, DMAN (**a**),[2] which has a pK_a of 18.62 in acetonitrile[3]) is the incorporation of more than one guanidino functionality in a single molecular species, with a corresponding increase in the sites at which cationic resonance can occur (provided a suitable pathway is available for charge transfer between units).

A series of bis-guanidino compounds is illustrated in Figure 1, including examples of both isolated (**b**, TMGB;[4] **c**, TMGN;[5] **d**, TMGBP;[6] and **e**, DMEGN[7]) and theoretical (**f**, TMGF;[8] and **g**, TMGBH[9]) molecules. Detailed structural, spectroscopic, and

† University of Sussex.
‡ University of Bath.
§ Rudjer Bošković Institute.
|| University of Tartu.
⊥ University of Durham.

(1) Maksić, Z. B.; Kovačević, B. *J. Org. Chem.* **2000**, *65*, 3303–3309.
(2) Alder, R. W.; Bowman, P. S.; Steele, W. R. S.; Winterman, D. R. *Chem. Commun. (London)* **1968**, 723–724.
(3) Kaljurand, I.; Kütt, A.; Sooväli, L.; Rodima, T.; Mäemets, V.; Leito, I.; Koppel, I. A. *J. Org. Chem.* **2005**, *70*, 1019–1028.
(4) (a) Kawahata, M.; Yamaguchi, K.; Ito, T.; Ishikawa, T. *Acta Crystallogr. E* **2006**, *62*, o3301–o3302. (b) Peters, A.; Wild, U.; Hübner, O.; Kaifer, E.; Himmel, H.-J. *Chem.—Eur. J.* **2008**, *14*, 7813–7821.
(5) Raab, V.; Kipke, J.; Gschwind, R. M.; Sundermeyer, J. *Chem.—Eur. J.* **2002**, *8*, 1682–1693.
(6) Pruszynski, P.; Leffek, K. T.; Borecka, B.; Cameron, T. S. *Acta Crystallogr. C* **1992**, *48*, 1638–1641.
(7) Raab, V.; Harms, K.; Sundermeyer, J.; Kovačević, B.; Maksić, Z. B. *J. Org. Chem.* **2003**, *68*, 8790–8797.
(8) Kovačević, B.; Maksić, Z. B. *Chem.—Eur. J.* **2002**, *8*, 1694–1702.

10.1021/ja906618g CCC: $40.75

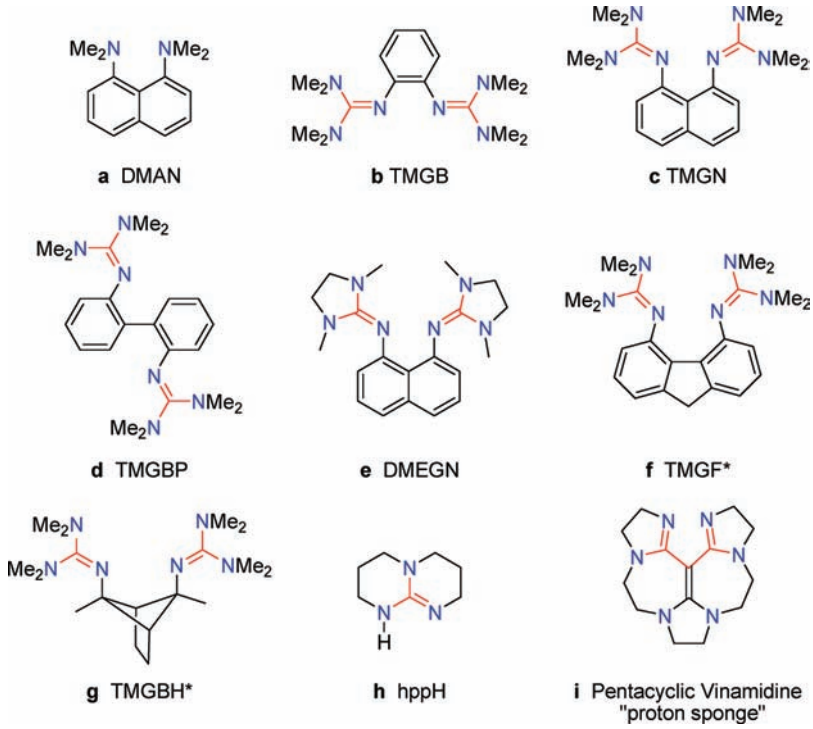

Figure 1. Superbases incorporating amine, amidine, and guanidine groups that have been previously studied (* denotes theoretical molecule only): 1,8-bis(dimethylamino)naphthalene (**a**, DMAN), 1,2-bis(tetramethylguanidino)benzene (**b**, TMGB), 1,8-bis(tetramethylguanidino)naphthalene (**c**, TMGN), 2,2′-bis(tetramethylguanidino)biphenyl (**d**, TMGBP), 1,8-bis(dimethylethyleneguanidino)naphthalene (**e**, DMEGN), 4,5-bis(tetramethylguanidino)fluorene (**f**, TMGF), 5,6-dimethyl-5,6-bis(tetramethylguanidino)bicyclo[2.1.1]hexane (**g**, TMGBH), 1,3,4,6,7,8-hexahydro-2*H*-pyrimido[1,2-*a*]pyrimidine (**h**, hppH), and pentacyclic "proton sponge" with vinamidine structure (**i**).

theoretical data have been presented,[10] leading to the conclusion that these molecules do indeed behave as superbases. Similar compounds were reported by Schwesinger, who employed vinamidine residues consisting of tricyclic[11] and pentacyclic (**i**)[12] poly(amidino) compounds.

The tetrasubstituted, bicyclic guanidine hppH (**h**)[13] represents the most widely used member of a family of bicyclic guanidines,[14] in which the framework of the guanidine is constrained such that, upon protonation, a favorable orbital alignment for delocalization of π-electron density is present. The interest for some of us in this molecule originated from its application as a neutral ligand in coordination chemistry,[15] where it was noted that metal−ligand interactions predominantly occurred through the N_{imine}. Extension to bidentate ligand systems that preserved the imino functionality was achieved in the examples $H_2C\{hpp\}_2$ (**I**)[16] and $Me_2Si\{hpp\}_2$.[17] NMR studies showed the silyl-bridged system was fluxional in solution while

Scheme 1. Nucleophilic Activity of $H_2C\{hpp\}_2$ (**I**)

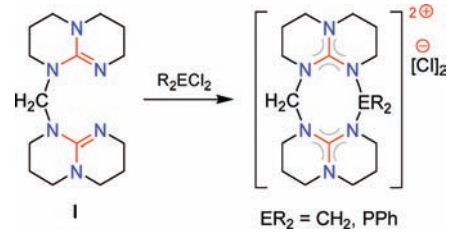

the carbon-bridged variant **I** provided a stable framework for further studies.

We have also noted that the reactivity of $H_2C\{hpp\}_2$ differs significantly from that of the parent guanidine. For example, nucleophilic behavior with organic[18] and inorganic[19] substrates affords the eight-membered, dicationic heterocycles $[H_2C\{hpp\}_2\text{-}\mathbf{X}]^{2+}$ ($\mathbf{X} = CH_2$ and PPh, Scheme 1). We have also investigated the ability of **I** to act as a ligand for cationic metals, illustrated by the stable aluminum cation $[AlMe_2(H_2C\{hpp\}_2)][BPh_4]$, accessed via a guanidinium salt containing monocation $[\mathbf{I}\text{-H}]^+$.[20] In this paper we present a detailed structural analysis of $[\mathbf{I}\text{-H}]^+$ in the solution and solid phases. These data are used in conjunction with computational studies to examine the basicity of $H_2C\{hpp\}_2$, the results of which are verified by experimental measurements. Anticipating forthcoming results, we should emphasize that the dominating structural and electronic pattern

(9) Singh, A.; Ganguly, B. *New J. Chem.* **2008**, *32*, 210–213.
(10) Ishikawa, T. Guanidines in Organic Synthesis. In *Superbases for Organic Synthesis*; Ishikawa, T., Ed.; Wiley-Blackwell: New York, 2009; pp 93−136.
(11) Schwesinger, R. *Angew. Chem., Int. Ed. Engl.* **1987**, *26*, 1164–1165.
(12) Schwesinger, R.; Missfeldt, M.; Peters, K.; von Schnering, H. G. *Angew. Chem., Int. Ed. Engl.* **1987**, *26*, 1165–1167.
(13) hppH is also referred to as 1,5,7-triazabicyclo[4.4.0]dec-5-ene, abbreviated to TBD. See ref 14 for a recent discussion of the nomenclature of bicyclic guanidines.
(14) Coles, M. P. *Chem. Commun.* **2009**, 3659–3676.
(15) (a) Coles, M. P. *Dalton Trans.* **2006**, 985–1001. (b) Oakley, S. H.; Soria, D. B.; Coles, M. P.; Hitchcock, P. B. *Polyhedron* **2006**, *25*, 1247–1255. (c) Oakley, S. H.; Soria, D. B.; Coles, M. P.; Hitchcock, P. B. *Dalton Trans.* **2004**, 537–546. (d) Oakley, S. H.; Coles, M. P.; Hitchcock, P. B. *Inorg. Chem.* **2003**, *42*, 3154–3156. (e) Coles, M. P.; Hitchcock, P. B. *Polyhedron* **2001**, *20*, 3027–3032.
(16) Oakley, S. H.; Coles, M. P.; Hitchcock, P. B. *Inorg. Chem.* **2004**, *43*, 7564–7566.
(17) Oakley, S. H.; Coles, M. P.; Hitchcock, P. B. *Dalton Trans.* **2004**, 1113–1114.
(18) Coles, M. P.; Lee, S. F.; Oakley, S. H.; Estiu, G.; Hitchcock, P. B. *Org. Biomol. Chem.* **2007**, *5*, 3909–3911.
(19) Coles, M. P.; Hitchcock, P. B. *Chem. Commun.* **2007**, 5229–5231.
(20) Aragón-Sáez, P. J.; Oakley, S. H.; Coles, M. P.; Hitchcock, P. B. *Chem. Commun.* **2007**, 816–818.

Scheme 2. Synthesis of Cationic Guanidinium Salts Examined in This Study: (a) $HNEt_3Cl$, CH_2Cl_2; (b) $NaBPh_4$, H_2O

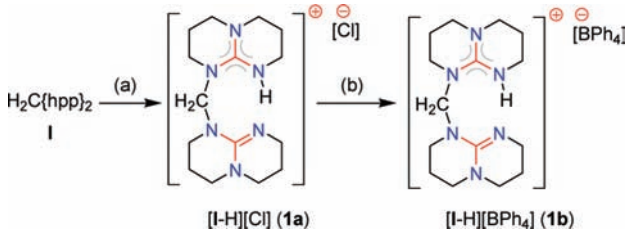

found in the protonated form of **I** is a cyclic, H-bond moiety used as a motif in designing organic superbases by a number of researchers.[21]

Monoprotonated Poly(guanidinium) Salts: $[I\text{-}H]^+[Anion]^-$

Synthesis and Spectroscopic Properties. Protonation of $H_2C\{hpp\}_2$ (**I**) using triethylamine hydrochloride in CH_2Cl_2 afforded the guanidinium salt, $[H_2C\{hpp\}\{hpp\text{-}H\}][Cl]$ ([**I**-H][Cl], **1a**), which was isolated as a hygroscopic white powder (Scheme 2). The ^1H NMR spectrum in acetonitrile showed a clearly defined broad singlet at δ 13.25 ppm, attributed to the N*H* proton. Previous work has denoted far downfield chemical shifts ($\delta \geq 15$ ppm) as indicative of the presence of strong hydrogen bonding, with for example hydrogen-bound imino protons in duplex and quadruplex DNA structures typically in the range δ 10−14 ppm.[22] The bridging methylene resonance is a sharp singlet at δ 4.77 ppm, and six multiplets are observed for the annular methylene groups, consistent with equivalent guanidino units. These data are inconsistent with a structure in which protonation has occurred exclusively at one nitrogen (**A**, Figure 2) and are in agreement with either a symmetric cation in which each ring is equally involved in hydrogen-bonding (**B**) or a fluxional system in which proton transfer between the protonated N*H* and the remaining N_{imine} occurs rapidly on the NMR time scale (**C**/**D**).

To improve the solubility of $[I\text{-}H]^+$, anion metathesis was performed with $NaBPh_4$ to afford the tetraphenylborate salt, $[I\text{-}H][BPh_4]$ (**1b**).[20] The room-temperature ^1H NMR spectrum is similar to that of **1a**, with a low-field resonance for the N*H* proton (δ 13.51 ppm), a sharp singlet for the bridging methylene group, and six hpp-methylene environments. The increased solubility of **1b** enabled low-temperature ^{13}C NMR spectra to be acquired on the $[I\text{-}H]^+$ cation. The lack of line broadening at 223 K provided further evidence for equivalence of the two guanidino groups in solution.

Solid-State Structure of $[H_2C\{hpp\}\{hppH\}]^+$ ($[I\text{-}H]^+$). To determine the structure of cation $[I\text{-}H]^+$ in the solid state, tetraphenylborate salt **1b** was investigated by solid-state NMR spectroscopy and X-ray crystallography. The CPMAS ^{13}C NMR experiment was not particularly informative, as the carbon atoms joined to nitrogen (i.e., all but one in the cation) were broadened through residual dipolar coupling to ^{14}N (Figure S2, Supporting Information). The CPMAS ^{15}N NMR spectrum, however, consisted of six distinct lines that, given there is only one molecule in the crystallographic unit cell (*vide infra*), establish

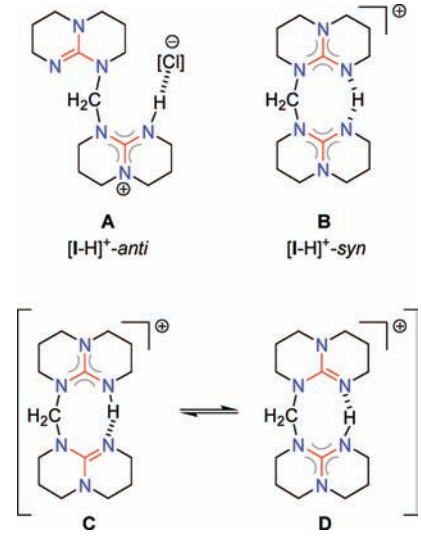

Figure 2. Possible solution-state structures for the monocation $[I\text{-}H]^+$.

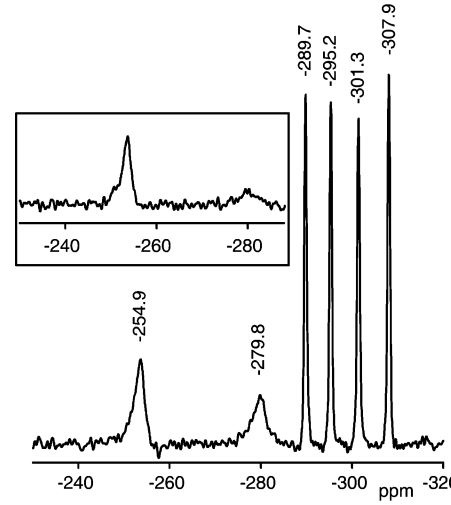

Figure 3. CPMAS ^{15}N NMR spectrum for $[H_2C\{hpp\}\{hppH\}][BPh_4]$ (**1b**). Inset: Results from a dipolar dephasing experiment, showing suppression of the peak at δ −279.8 ppm.

that the two rings are inequivalent (Figure 3). The four narrow lines have a full width at half-height (fwhh) of ∼14 Hz and are assigned to the four tertiary nitrogen atoms. The remaining two signals at δ −254 and −280 ppm are broader (fwhh = 66 and 83 Hz, respectively), which suggests that each atom experiences an interaction with ^1H. The different chemical shifts and line widths, however, show that the $^{15}N-^1H$ interaction is not equal for each nitrogen involved. This is consistent with an asymmetric intramolecular hydrogen bond (IHB) of the form $[N—H\cdots N']^+$ (i.e., **C** or **D**), previously documented in other poly(guanidino) compounds,[5,7] or may be indicative of solid-state proton transfer (SSPT), previously observed in examples of amidine[23] and guanidine[24] dimers.

A dipolar dephasing experiment was performed (inset, Figure 3), showing that the line at δ −254 ppm loses very little intensity

(21) (a) Raczyńska, E. D.; Decouzon, M.; Gal, J.-F.; Maria, P.-C.; Gelbard, G.; Vielfaure-Joly, F. *J. Phys. Org. Chem.* **2001**, *14*, 25–34. (b) Tian, Z.; Fattahi, A.; Lis, L.; Kass, S. R. *Croat. Chem. Acta* **2009**, *82*, 41–45.
(22) Engelhart, A. E.; Morton, T. H.; Hud, N. V. *Chem. Commun.* **2009**, 647–649.
(23) (a) Anulewicz, R.; Wawer, I.; Krygowski, T. M.; Männle, F.; Limbach, H.-H. *J. Am. Chem. Soc.* **1997**, *119*, 12223–12230. (b) Lopez, J. M.; Männle, F.; Wawer, I.; Buntkowsky, G.; Limbach, H.-H. *Phys. Chem. Chem. Phys.* **2007**, *9*, 4498–4513.
(24) Coles, M. P.; Khalaf, M. S.; Claramunt, R. M.; García, M. A.; Alkorta, I.; Elguero, I. *J. Phys. Org. Chem.* **2009**, DOI: 10.1002/poc.1636.

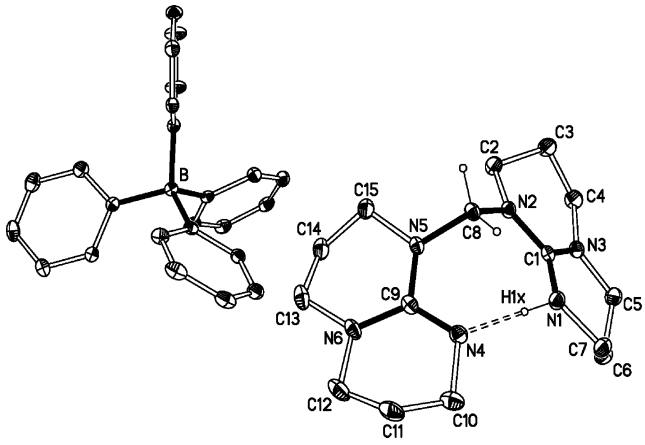

Figure 4. Thermal ellipsoid plot (20%) of $[H_2C\{hpp\}\{hppH\}][BPh_4]$ (**1b**) at 173(2) K. Hydrogen atoms, except NH and those on the bridging methylene group, are omitted.

but that the δ −280 ppm resonance is almost fully suppressed. This indicates that one nitrogen is largely tertiary in character and the other corresponds to an *N*H group, in agreement with the asymmetry proposed above. In an attempt to ascertain whether exchange of the proton between the two nitrogen positions of the bridge was occurring in the solid state, EXSY experiments were performed using both long (200 ms) and short (30 ms) mixing times. However, no cross-peaks were identified in either experiment, indicating that, if exchange is taking place, it cannot be detected in this system using this technique.

X-ray diffraction data for **1b** at 173(2) K showed a noncontacted ion pair with an IHB in the cationic component (Figure 4),[20] in agreement with the solution- and solid-state NMR data. The N1···N4 distance, 2.73 Å, is long compared with the corresponding values for $[TMGN-H]^+$ and $[DMEGN-H]^+$, in which the two nitrogen atoms are in the 1,8-positions of a rigid naphthalene framework (average N···N′ separation of 2.59 Å).[5,7] Accordingly the N*H* atom in **1b** was located, refined, and shown to be associated with only one nitrogen atom in an asymmetric IHB, with a relatively linear bridge angle of 167° (cf. 152° and 142° for $[TMGN-H]^+$ and $[DMEGN-H]^+$, respectively). We note, however, that the N···N′ distance alone cannot be used to determine whether a single minimum is present. For example, N*H* disorder is observed in the cyclic *N*,*N*,*N*′,*N*′-tetramethylputrescine cation, with N···N′ of 2.66 Å,[25] while in even shorter NH···N′ interactions, for example 2.526(3) Å in 1,6-diazabicyclo[4.4.4]tetradecane,[26] an element of doubt concerning the position of the proton remains.

X-ray diffraction data for **1b** have been collected at 293(2), 173(2), 110(2), and 50(2) K (Tables 1 and S1, Supporting Information), and bond lengths associated with the IHB have been examined using previously defined parameters (Figure 5).[27]

The Δ_{CN} values[28] calculated for the protonated guanidino group of **1b** were less than that of the neutral precursor (Δ_{CN} = 0.106 Å for **I** at 173(2) K[18]), in accord with the expected increase in delocalization upon protonation (Figure 6). We note, however, that the Δ_{CN} value of the formally neutral guanidino group in **1b** is also less than that of the fully localized system **I**, consistent with some degree of delocalization attributed to "partial protonation" of this component.[8] As the temperature was lowered, Δ_{CN}(protonated) decreased with a concurrent

Table 1. Selected Bond Lengths (Å) for **1b**, Taken from Data Collected at 273(2), 173(2), 110(2), and 50(2) K

	273(2) K	173(2) K	110(2) K	50(2) K
C1−N1	1.316(3)	1.326(2)	1.3406(10)	1.335(2)
C1−N2	1.350(3)	1.357(2)	1.3623(9)	1.350(2)
C1−N3	1.348(3)	1.341(2)	1.3489(9)	1.336(2)
C9−N4	1.304(3)	1.300(2)	1.3070(10)	1.300(2)
C9−N5	1.377(3)	1.384(2)	1.3946(10)	1.385(2)
C9−N6	1.356(3)	1.362(2)	1.3683(10)	1.363(2)
N1···N4	2.71	2.73	2.75	2.73
		Protonated Group		
Δ_{CN}	0.034	0.031	0.022	0.015
Δ'_{CN}	0.015	0	−0.003	−0.007
ρ-ratio	0.976	0.983	0.989	0.994
		Neutral Group		
Δ_{CN}	0.073	0.084	0.088	0.085
Δ'_{CN}	0.016	0.020	0.018	0.021
ρ-ratio	0.954	0.947	0.946	0.946

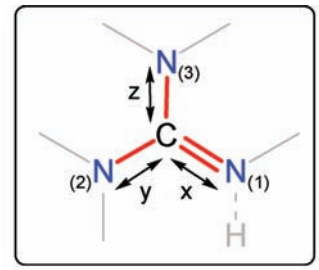

$$\Delta_{CN} / Å = y - x$$

$$\Delta'_{CN} / Å = z - [\{x + y\} / 2]$$

$$\rho = 2x / (y + z)$$

Figure 5. Structural parameters used to describe bonding in guanidines.

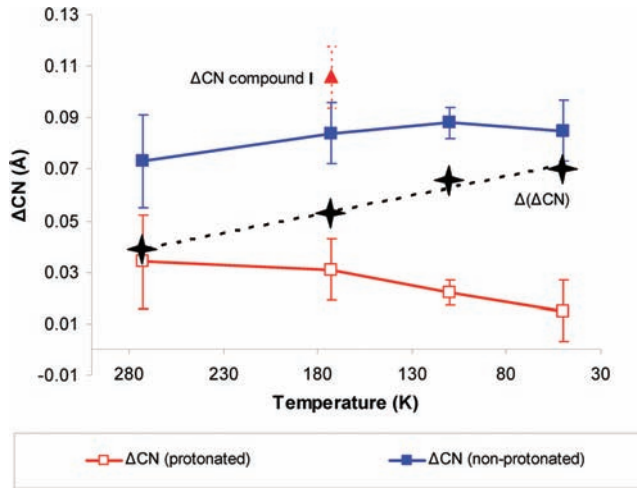

Figure 6. Graphical representation of differences in Δ_{CN} with temperature. The red triangle represents the value of the neutral precursor compound, $H_2C\{hpp\}_2$ (**I**). $\Delta(\Delta_{CN})$ is taken as the difference Δ_{CN}(nonprotonated) − Δ_{CN}(protonated); error bars are plotted at the 3σ level.

(25) Yaghmaei, S.; Khodagholian, S.; Kaiser, J. M.; Tham, F. S.; Mueller, L. J.; Morton, T. H. *J. Am. Chem. Soc.* **2008**, *130*, 7836–7838.
(26) Alder, R. W.; Orpen, A. G.; Sessions, R. B. *J. Chem. Soc., Chem. Commun.* **1983**, 999–1000.
(27) Khalaf, M. S.; Oakley, S. H.; Coles, M. P.; Hitchcock, P. B. *Cryst. Eng. Commun.* **2008**, *10*, 1653–1661.
(28) Häfelinger, G.; Kuske, F. K. H. *The Chemistry of Amidines and Imidates;* Wiley: Chichester, 1991.

Scheme 3. Cationic Resonance Stabilization for the "[∼hppH]$^+$" Guanidinium Group

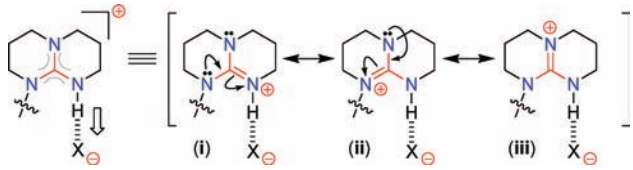

increase in Δ_{CN}(nonprotonated), resulting in a steady increase in the difference between these two values, $\Delta(\Delta_{CN})$ in Figure 6.

To gauge the contribution of the lone pair of atoms N3 and N6 to the overall bonding, the Δ'_{CN} value has been defined.[29] For compound **I**, $\Delta'_{CN} = 0.037$ Å,[18] indicating a relatively low degree of lone-pair delocalization from the tertiary nitrogen. A reduction of this value is observed in both guanidino groups in **1b**, with the largest reduction in Δ'_{CN}(protonated), consistent with greater overall contribution from the resonance form **iii** (Scheme 3) to offset the positive charge in this group.

Another parameter used when describing the bonding in guanidines is the ρ-ratio, defined as a measure of the elongation of the C═N double bond on protonation, relative to the concomitant shortening of the average C−NR_2 distance (Figure 5).[7,8] The ρ-ratio for $H_2C\{hpp\}_2$ is 0.929,[30] indicating that the C═N double bond length is equal to 92.9% of the average C−NR_2 bond distance. While no clear temperature dependence is noted for the ρ-ratio in **1b**, the larger values for the protonated group (97.6−99.4%) are consistent with more efficient delocalization when compared with **I**, in fitting with the Δ'_{CN} values. The corresponding values of ρ for the nonprotonated guanidino group (94.6−95.4%) are also indicative of a lengthened C═N double bond compared with that in **I**, giving further structural evidence for partial protonation of the second guanidino group.

It is important to note that the Δ_{CN}, Δ'_{CN}, and ρ value ranges for the formally neutral guanidino component of **1b** are intermediate between those of the protonated group and the corresponding values for **I**. The presence of a (nondetectable) static disorder in the N*H* position, which is associated with N4 rather than N1 in the minor component, would account for the observed differences in bond length averages reported in the crystal structures. However, the regular trends observed as the temperature is varied suggest a dynamic process which, in agreement with CPMAS ^{15}N NMR data, is consistent with SSPT between N1 and N4. Furthermore, a decrease in the rate of proton transfer as the temperature is lowered would be expected, resulting in a seemingly more ordered system and an increased $\Delta(\Delta_{CN})$, as noted in the X-ray diffraction data (Figure 6).

To directly observe the proton transfer between atoms N1 and N4, difference electron density maps were calculated from high-resolution X-ray diffraction data acquired at 110(2) K (Figure 7). At higher temperatures the proton is able to shuttle between the two nitrogens at a faster rate. Indeed, the 110(2) K data indicate electron density at the correct distance for an N(4)−H component of **1b** (peak ∼0.18 e Å^{-3}), commensurate with the incipient stage of the proton transfer to the second guanidino group. To our knowledge, this is the first time that this phenomenon has been directly detected experimentally, in contrast to previous studies, in which this process is inferred from perturbations of other bonds within the molecule, and the present calculations, which predict a very low barrier height for the proton transfer (see later).

Computational Analysis. The calculations have been carried out at the DFT level using the Gaussian 03 suite of programs.[31] The optimal gas-phase structures of the neutral species $H_2C\{hpp\}_2$ (**I**) and the *N*-methylated compound hppMe (**II**) along with their conjugate acids, $[H_2C\{hpp\}\{hppH\}]^+$ ([**I**-H]$^+$) and [hppMe-H]$^+$ ([**II**-H]$^+$), have been computed using the B3LYP/6-31G(d) method (Figure 8). In the neutral form, **II** displays a typical distribution of carbon−nitrogen bond lengths within the guanidino portion of the molecule, with a relatively large Δ_{CN} (0.11 Å) indicating a localized bonding pattern with little contribution from the lone pair at N3 ($\Delta'_{CN} = 0.05$ Å). Upon protonation at the imine nitrogen, changes in the guanidino C−N bond lengths indicate strong cationic resonance stabilization (Scheme 3), reflected in the new Δ_{CN}, Δ'_{CN}, and ρ-values. A very similar distribution of bond lengths is noted for bisguanidino **I**, implying that the presence of the second functionality does not significantly alter the geometric parameters of the constituent fragments.

The optimized geometries for [**I**-H]$^+$ indicate that the protonated guanidino group is subject to cationic resonance stabilization, although to a lesser extent than observed for [**II**-H]$^+$. This can be seen in the larger Δ_{CN} (0.03 Å) and Δ'_{CN} (0.01 Å) values compared with the corresponding values for [**II**-H]$^+$ (0.00 and −0.01 Å, respectively). For the formally neutral guanidino group in [**I**-H]$^+$, the C═N bond (1.304 Å) shows a significant increase compared with the value for either **I** (1.298 Å) or **II** (1.292 Å); in the same vein, the C−N bonds involving the tertiary nitrogen atoms are significantly shortened upon protonation. In [**I**-H]$^+$, however, the correspondingly large increase in the C−N single bond from 1.387 Å in **I** to 1.402 Å in the cation implies that cationic resonance does not use all possible pathways in the partially protonated fragment. The reduction in Δ'_{CN} and increase in the ρ-ratio for the formally nonprotonated guanidino group are nevertheless strong evidence that protonation of one guanidino unit promotes partial protonation of the second guanidino framework. This is also evidenced by the longer N$^+$−H bond of 1.064 Å in [**I**-H]$^+$ compared with 1.009 Å in [**II**-H]$^+$. Finally we note the hydrogen bond angle in [**I**-H]$^+$ of 176.9°, close to the ideal linear arrangement that is a prerequisite of a strong hydrogen-bonding interaction.

Results from natural bond orbital analysis[32] show the atomic charges of N1, N2, and N3 to be greater than their counterparts in the nonprotonated guanidino group, indicating that the positive charge is predominantly located on these atoms (Figure 9a). Second-order perturbation theory shows that, in the nonprotonated guanidino group, significant stabilization energies of 51.8 and 63.5 kcal mol^{-1} arise from delocalization of the N5 and N6 lone pairs into the antibonding orbital of the imine bond (π^* C9−N4) and are similar in magnitude to those in hppH (57.4 and 55.8 kcal mol^{-1}).[33] In the protonated group, these stabilizing effects are more pronounced due to the greater charge, with the corresponding energies calculated as 76.8 and 84.3 kcal mol^{-1}, respectively. We also note a significant stabilization of 40.1 kcal mol^{-1} derived from projection of the N4 lone pair into the σ^* orbital of the N−H bond.

(29) Coles, M. P.; Hitchcock, P. B. *Organometallics* **2003**, *22*, 5201–5211.
(30) The ρ-ratio for $H_2C\{hpp\}_2$ was incorrectly reported as 0.89 in ref 27.
(31) Frisch, M. J.; et al. *Gaussian 03*, revision 03W; Gaussian Inc.: Wallingford, CT, 2004.
(32) Foster, J. P.; Weinhold, F. *J. Am. Chem. Soc.* **1980**, *102*, 7211–7218.
(33) Khalaf, M. S.; Coles, M. P.; Hitchcock, P. B. *Dalton Trans.* **2008**, 4288–4295.

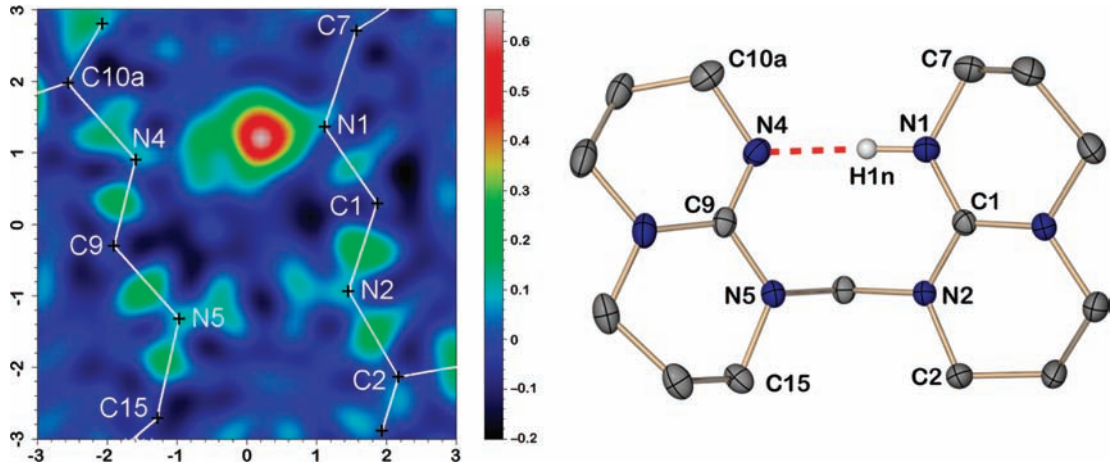

Figure 7. Difference electron density map (min, −0.23 e Å^{-3}; max, 0.83 e Å^{-3}) for the hydrogen-bonding region of **1b** at 110 K, showing the position of H1n, with evidence for partial protonation of N4.

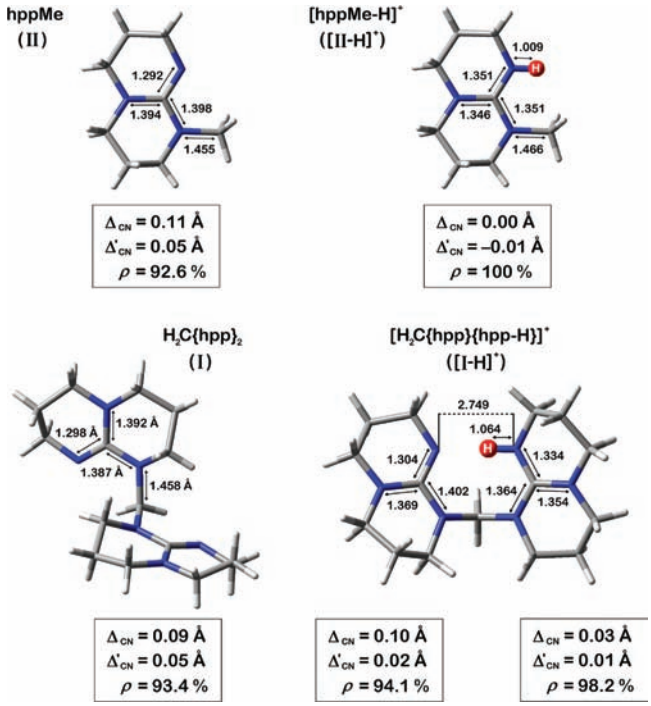

Figure 8. Summary of key structural data from DFT analysis of **II**, [**II**-H]$^+$, **I**, and [**I**-H]$^+$ in the gas phase (note that the two guanidino groups in **I** are related by symmetry).

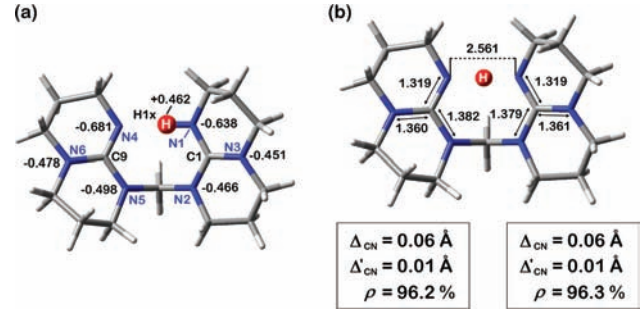

Figure 9. (a) Natural atomic charges on key atoms of [**I**-H]$^+$. (b) Summary of key structural data from DFT analysis of [**I**-H]$^+$-**TS**.

The transition state for the interconversion of the different tautomers (**C/D**) was located on the potential surface ([**I**-H]$^+$-**TS**), consisting of a single negative frequency corresponding to the N—H···N ↔ N···H—N vibration (Figure 9b). A reorganization of π-electron density within both guanidino functionalities accompanies the proton-transfer process, resulting in a nearly symmetrical structure for [**I**-H]$^+$-**TS**. The Δ_{CN}, Δ'_{CN}, and ρ-values reflect an increased delocalization in the formerly neutral guanidino group, with a concomitant reduction in the formerly protonated group, making them almost equivalent. The N—H$^+$ distance of the hydrogen bridge in the equilibrium structure of [**I**-H]$^+$ is increased by 0.218 Å on going to the TS position in [**I**-H]$^+$-**TS**. It is surprising that such a small step for the positively charged H$^{\delta+}$ atom leads to such a large change in the electronic and spatial structure of both fragments.

The gas-phase barrier for proton transfer (calculated as the difference in electronic energy between the transition state and the equilibrium ground state) is +2.5 kcal mol^{-1}, somewhat higher than that reported for 1,8-bis(dimethylamino)naphthalene-2,7-diolate (+0.9 kcal mol^{-1})[34] and the corresponding 2,7-dimethoxy-substituted proton sponge (+1.4 kcal mol^{-1})[35] but identical to the value for the protonated 8-aminoguanine dimer (+2.5 kcal mol^{-1}).[22] A significant reduction in the N···N distance is noted in [**I**-H]$^+$-**TS** (2.561 Å; cf. 2.749 Å in the ground state), with the hydrogen atom positioned with the N···H···N angle 177.3°. To validate this result, the computations were repeated by the Boese−Martin for kinetics (BMK) method,[36] which is advocated as the best DFT approach for estimating the barrier heights. The corresponding barrier is almost the same, being 2.7 kcal mol^{-1} at the BMK/6-311+G(2df,p)//B3LYP/6-31G(d) level of theory and 2.8 kcal mol^{-1} as obtained by the BMK/6-311+G(2df,p)//BMK/6-31G(d) method. Therefore, it is gratifying that a more widely used DFT functional, namely B3LYP, is able to accurately predict barrier heights for the proton-transfer reactions within a few tenths of a kcal mol^{-1} from the BMK results. However, explicit inclusion of zero-point vibrational energy (ZPVE) values, obtained at the B3LYP/6-31G(d) level of theory, removes the barrier for the proton transfer. More precisely, the difference in the unscaled ZPVE values between the transition-state structure [**I**-H]$^+$-**TS**

(34) Ozeryanskii, V. A.; Milov, A. A.; Minkin, V. I.; Pozharskii, A. F. *Angew. Chem., Int. Ed.* **2006**, *45*, 1453–1456.
(35) Ozeryanskii, V. A.; Pozharskii, A. F.; Bieńko, A. J.; Sawka-Dobrowlska, W.; Sobczyk, L. *J. Phys. Chem. A* **2005**, *109*, 1637–1642.
(36) Boese, A. D.; Martin, J. M. L. *J. Chem. Phys.* **2004**, *121*, 3405–3416.

Table 2. Calculated Basicity Constants for the Molecules of Interest in This Study

compound	PA (gas phase) (kcal mol^{-1})	pK_a (MeCN)	IHB[a](kcal mol^{-1})	ref
$H_2C\{hpp\}_2$ (**I**)	270.6[b]	28.6		this work
$[H_2C\{hpp\}\{hppH\}]^+$ $[\mathbf{I}\text{-H}]^+$	176.7[b]	17.8	14.8	this work
hppMe (**II**)	255.8[b]	25.3		this work
DMAN (**a**)	245.1	19.9		37a
TMGB (**b**)	254.3[c]	24.0		37b
TMGN (**c**)	257.5[c]	25.4		8
$[\text{TMGN-H}]^+$ ($[\mathbf{c}\text{-H}]^+$)	178.7[c]		12.5	8
TMGBP (**d**)	263.8[c]	25.9		37b
DMEGN* (**e**)	250.8[c]	23.0		7
DMEGN† (**e′**)	250.8[c]	22.4		7
$[\text{DMEGN*-H}]^+$ ($[\mathbf{e}\text{-H}]^+$)			9.2	7
TMGF (**f**)	263.7[c]	27.8		8
$[\text{TMGF-H}]^+$ ($[\mathbf{f}\text{-H}]^+$)			17.6	8
TMGBH (**g**)	273.8[d]			9

[a] Calculated from the relevant homodesmotic reactions. [b] B3LYP/6-311+G(2df,p)//B3LYP/6-31G(d) model. [c] MP2(fc)/6-311+G(d,p)//HF/6-31G(d) model. [d] B3LYP/6-311+G(d,p)//B3LYP/6-31+G(d) model. In the first column, the * indicates *syn*-DMEGN and the † indicates *anti*-DMEGN.

and the ground-state protonated molecule $[\mathbf{I}\text{-H}]^+$ is -2.7 kcal mol^{-1}. This implies that ZPVE in the transition-state structure is lower than that in the ground state, since there is one vibration with imaginary frequency of -1118.7 cm^{-1}, which is not contributing to the ZPVE in the former system. Therefore, we conclude that the proton transfer in the monoprotonated compound $[\mathbf{I}\text{-H}]^+$ is barrierless and that the proton shuttles freely between the two imino nitrogens, leading to two equivalent guanidino moieties, if averaged over the longer time.

Basicity Studies

Calculated Proton Affinities in the Gas Phase and in Acetonitrile Solution. To examine the basicity of the molecules described in this study, we have performed additional theoretical studies on **I** and $[\mathbf{I}\text{-H}]^+$ in the gas phase and in acetonitrile solution, involving the two different conformers $[\mathbf{I}\text{-H}]^+$-*syn* and $[\mathbf{I}\text{-H}]^+$-*anti*. The basicity constants for the molecules of interest are presented in Table 2, along with those of the bis-guanidino compounds from Figure 1.[7−9,37] It is reassuring to note that the gas-phase proton affinity (PA) for hppMe (**II**) calculated during this study (255.8 kcal mol^{-1}) is in good agreement with the experimentally determined value of 254.0 kcal mol^{-1}.[38] This gives a theoretical estimate within chemical accuracy of ± 2.0 kcal mol^{-1}, lending credibility to the other predicted values presented in this study.

Monoprotonation of **I** to give cation $[\mathbf{I}\text{-H}]^+$ has an associated proton affinity (PA) of 270.6 kcal mol^{-1}. This is considerably greater than those of the related bis-guanidino compounds in Table 2 and a series of hypothetical bis(tetramethylguanidino) systems supported by a range of rigid backbones (range 241−268 kcal mol^{-1}). Similarly high PAs (up to 275.5 kcal mol^{-1}) have been calculated for 3-aminopropyl-substituted *N*,*N*′,*N*″-trimethylguanidines, with such high values in this instance attributed to strong cationic resonance within the central guanidine moiety, enhanced through the cooperative multiple intramolecular hydrogen bonding.[39] Given that the cation $[\mathbf{I}\text{-H}]^+$ has an observed IHB in the solid state that is believed to be maintained in solution, we wished to examine the role that this interaction plays on the high PA value. It is useful to note that the gas-phase basicities (GBs) of **I** and **II** are 261.8 and 248.5 kcal mol^{-1}, respectively.

A useful method for exploring the interaction between different fragments derives from the concept of homodesmotic reactions,[40] from which we obtain eqs 1−3. The difference of these equations gives the relationship PA(**I**) − PA(**II**) = $-(E_1 - E_2)$, which shows that **I** has larger PA than **II** by 14.8 kcal mol^{-1} since the energies E_1 and E_2 are 6.7 and 21.5 kcal mol^{-1}, respectively. This difference can be attributed to the hydrogen bond energy in $[\mathbf{I}\text{-H}]^+$. Compared with values for the related systems in Table 2 and a series of published diamines (for which it was calculated that the IHB contributed 10−17 kcal mol^{-1} to the GB),[41] the IHB in $[\mathbf{I}\text{-H}]^+$ may be considered relatively strong.

In contrast to most systems investigated using these techniques, for which the framework holding the two guanidino moieties is rigid, the conformational flexibility of **I** has enabled this result to be tested by calculating the PA for **I** with a conformation of the conjugate acid that does not lead to formation of a linear IHB (eq 3). For compound **I** this is the $[\mathbf{I}\text{-H}]^+$-*anti* conformation, in which the protonated guanidino fragment is rotated about the central methylene unit (Figure 2). The proton affinity for this conformation, PA′(**I**), is 261.9 kcal mol^{-1}, giving a difference in the values calculated for the two conformations of $[\mathbf{I}\text{-H}]^+$ of 8.7 kcal mol^{-1}. This is in harmony with the result obtained for eq 3, $E_3 = 12.8$ kcal mol^{-1}, smaller than E_2 by approximately 50%. The difference between eqs 1 and 3 gives a H$^+$-bond strength in $[\mathbf{I}\text{-H}]^+$-*anti* of 6.1 kcal mol^{-1}, which is a consequence of the interaction between the proton attached to the imino nitrogen N1 and a lone pair of the N5(sp^3) atom. This N1−H$^+$···N5 hydrogen bond has an angle of 137.8°. The nonprotonated guanidine fragment is not stabilized by the cationic resonance, because the H-bond acceptor atom N5 is linked to the rest of the guanidine moiety by a N−C single bond. The latter acts as an "insulator" for the cationic resonance.[1] This is another reason why the N1−H$^+$···N5 hydrogen bond is weaker, in addition to its pronounced nonlinearity.

(37) (a) Kurasov, L. A.; Pozharskii, A. F.; Kumenko, V. V. *Zh. Org. Khim.* **1983**, *19*, 859–864. (b) Kovaćević, B.; Maksić, Z. B.; Vianello, R.; Primorac, M. *New J. Chem.* **2002**, *26*, 1329–1334.

(38) Lias, S. G. In *NIST Chemistry WebBook*; Linstrom, P. J., Mallard, W. G., Eds.; National Institute of Standards and Technology: Gaithersburg MD, June 2005; http://webbook.nist.gov/chemistry/.

(39) (a) Kovačević, B.; Glasovac, Z.; Maksić, Z. B. *J. Phys. Org. Chem.* **2002**, *15*, 765–774. (b) Glasovac, Z.; Kovačević, B.; Meštrović, E.; Eckert-Maksić, M. *Tetrahedron Lett.* **2005**, *46*, 8733–8736.

(40) (a) George, P.; Trachtman, M.; Bock, C. W.; Brett, A. M. *Tetrahedron* **1976**, *32*, 317–323. (b) George, P.; Trachtman, M.; Bock, C. W.; Brett, A. M. *J. Chem. Soc., Perkin Trans. 2* **1976**, 1222–1227.

(41) Rõõm, E.-I.; Kütt, A.; Kaljurand, I.; Koppel, I.; Leito, I.; Koppel, I. A.; Mishima, M.; Goto, K.; Miyahara, Y. *Chem.—Eur. J.* **2007**, *13*, 7631–7643.

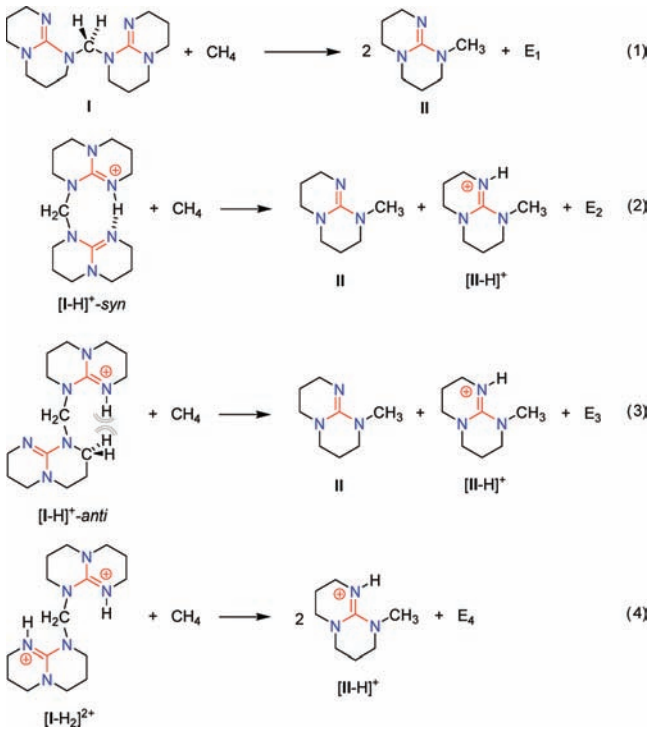

The protonation of $[\mathbf{I}\text{-H}]^+$ leading to the dication $[\mathbf{I}\text{-H}_2]^{2+}$ has a second PA considerably lower than the first, with a calculated value of only 176.7 kcal mol^{-1}. The corresponding homodesmotic reaction related to the diprotonated system $[\mathbf{I}\text{-H}_2]^{2+}$ is given in eq 4. In this model, E_4 essentially reflects repulsion when two protonated $[\mathbf{II}\text{-H}]^+$ fragments are combined in the diprotonated base $[\mathbf{I}\text{-H}_2]^{2+}$, with a value as high as −57.6 kcal mol^{-1}. If the difference between eqs 4 and 2 is taken, one obtains eq 5, where PA($[\mathbf{I}\text{-H}]^+$) is the second proton affinity yielding diprotonated form $[\mathbf{I}\text{-H}_2]^{2+}$.

$$\mathrm{PA}([\mathbf{I}\text{-H}]^+) = \mathrm{PA}(\mathbf{II}) + E_4 - E_2 \quad (5)$$

It appears that the second proton affinity, PA($[\mathbf{I}\text{-H}]^+$), is given by the proton affinity of the fragment **II** corrected by the repulsion energy E_4 and by the negative of E_2, because the stabilizing IHB occurring in the monoprotonated species is no longer present. The latter component is due to the fact that the second bridgehead nitrogen, which served as a hydrogen-bond acceptor in $[\mathbf{I}\text{-H}]^+$, is also protonated in the $[\mathbf{I}\text{-H}_2]^{2+}$ molecule.

The estimated basicity values in acetonitrile are also presented in Table 2. The difference in the gas-phase proton affinities between **I** and **II** (14.8 kcal mol^{-1}) yields a difference of only 3.3 pK_a units in MeCN. This is predominantly due to the inability of the protonation center to be efficiently solvated (stabilized) in $[\mathbf{I}\text{-H}]^+$ because of the strong IHB. These calculations have demonstrated that **I** can be classified as a strong superbase according to the gas-phase proton affinity of 270.6 kcal mol^{-1} and the corresponding pK_a value of 28.6, which is in good accordance with the experimentally determined value (see later).

Study of the Gas-Phase Basicity of I Using the Triadic Formula. To shed more light on the extremely high gas-phase basicity of $H_2C\{hpp\}_2$, we have used the recently proposed triadic formula,[42] which has previously been used to interpret Brønsted basicities[43] and acidities[44] and has been shown to have certain advantages over some other models.[45] Considering basicity, triadic analysis gives the gas-phase proton affinity of a base B according to eq 6:

$$\mathrm{PA(B)} = -\mathrm{IE(B)}_n^{\mathrm{Koop}} + E(\mathrm{ei})^{(n)}_{\mathrm{rex}} + (\mathrm{BAE})^{\bullet+} + 313.6\ \mathrm{kcal\ mol}^{-1} \quad (6)$$

This approach separates the protonation of a neutral organic base B into three sequential stages: (a) ionization of B by removal of an electron, generating a radical cation, (b) attachment of the ejected electron to the incoming proton to form the hydrogen atom (the released energy of 313.6 kcal mol^{-1} corresponds to the electron affinity of the proton),[38] and (c) creation of the chemical bond between the newly formed radical cation of the base and the hydrogen atom.

The initial state implies that the properties of the neutral base, B, and the effects on gas-phase basicities are reflected in Koopmans' ionization energies,[46] $\mathrm{IE(B)}_n^{\mathrm{Koop}}$, calculated in the frozen electron density and clamped atomic nuclei approximation. The $\mathrm{IE(B)}_n^{\mathrm{Koop}}$ values reflect the energy cost of taking an electron from the neutral molecule in a bond association with the incoming proton, assuming ionization is an instantaneous process, and since these energies depend exclusively on electron distribution throughout B described by molecular orbitals (MOs), they reflect genuine properties of the initial state. The orbitals undergoing ionization are called principal molecular orbitals (PRIMOs).

In the second intermediate step, the cation radical is allowed to fully relax in real time. The corresponding geometric and electronic reorganization effects following ejection of the electron are given by the relaxation energy $E(\mathrm{ei})^{(n)}_{\mathrm{rex}}$, defined by eq 7, where $\mathrm{IE(B)}_1^{\mathrm{ad}}$ is the first adiabatic ionization energy of the base.

$$E(\mathrm{ei})^{(n)}_{\mathrm{rex}} = \mathrm{IE(B)}_n^{\mathrm{Koop}} - \mathrm{IE(B)}_1^{\mathrm{ad}} \quad (7)$$

Finally, the bond association energy describing the homolytic bond formation between created radicals is given by the $(\mathrm{BAE})^{\bullet+}$ term, which represents features of the conjugate acid $[\mathrm{B-H}]^+$.

The results from the triadic analysis of **I**, $[\mathbf{I}\text{-H}]^+$-*syn*, and **II** are presented in Table 3. We have previously determined the

Table 3. Results Obtained from the Triadic Analysis of the Basicity of **I**, $[\mathbf{I}\text{-H}]^+$, and **II**

molecule (B)	$\mathrm{IE(B)}_n^{\mathrm{Koop}a}$	$\mathrm{IE(B)}_1^{\mathrm{ad}}$	$E(\mathrm{ei})^{(n)}_{\mathrm{rex}}$	$(\mathrm{BAE})^{\bullet+}$	PA(B)	$\mathrm{PA(B)}_{\mathrm{exp}}{}^b$
I	$(233.1)_5$	147.2	85.9	104.1	270.5	
$[\mathbf{I}\text{-H}]^+$	$(311.2)_3$	233.2	78.0	96.2	176.6	
II	$(232.9)_3$	158.1	74.8	100.2	255.7	254.0
PA(**I**) − PA(**II**)	−0.2		11.1	3.9	14.8	
PA($[\mathbf{I}\text{-H}]^+$) − PA(**I**)	−78.1		−7.9	−7.9	−93.9	

[a] The numerical subscripts n indicate the principal molecular orbital (PRIMO) in such a way that $n = 1$ represents the HOMO, $n = 2$ represents the HOMO−1, and so on. [b] Experimental data are taken from ref 37.

(42) Maksić, Z. B.; Vianello, R. *Pure Appl. Chem.* **2007**, *79*, 1003–1021.
(43) (a) Maksić, Z. B.; Vianello, R. *J. Phys. Chem. A* **2002**, *106*, 419–430. (b) Vianello, R.; Maskill, H.; Maksić, Z. B. *Eur. J. Org. Chem.* **2006**, 2581–2589. (c) Despotović, I.; Maksić, Z. B.; Vianello, R. *Eur. J. Org. Chem.* **2007**, 3402–3413.
(44) Maksić, Z. B.; Vianello, R. *ChemPhysChem* **2002**, *3*, 696–700.
(45) Deakyne, C. A. *Int. J. Mass Spectrom.* **2003**, *227*, 601–616.
(46) Koopmans, T. *Physica* **1933**, *1*, 104–113.

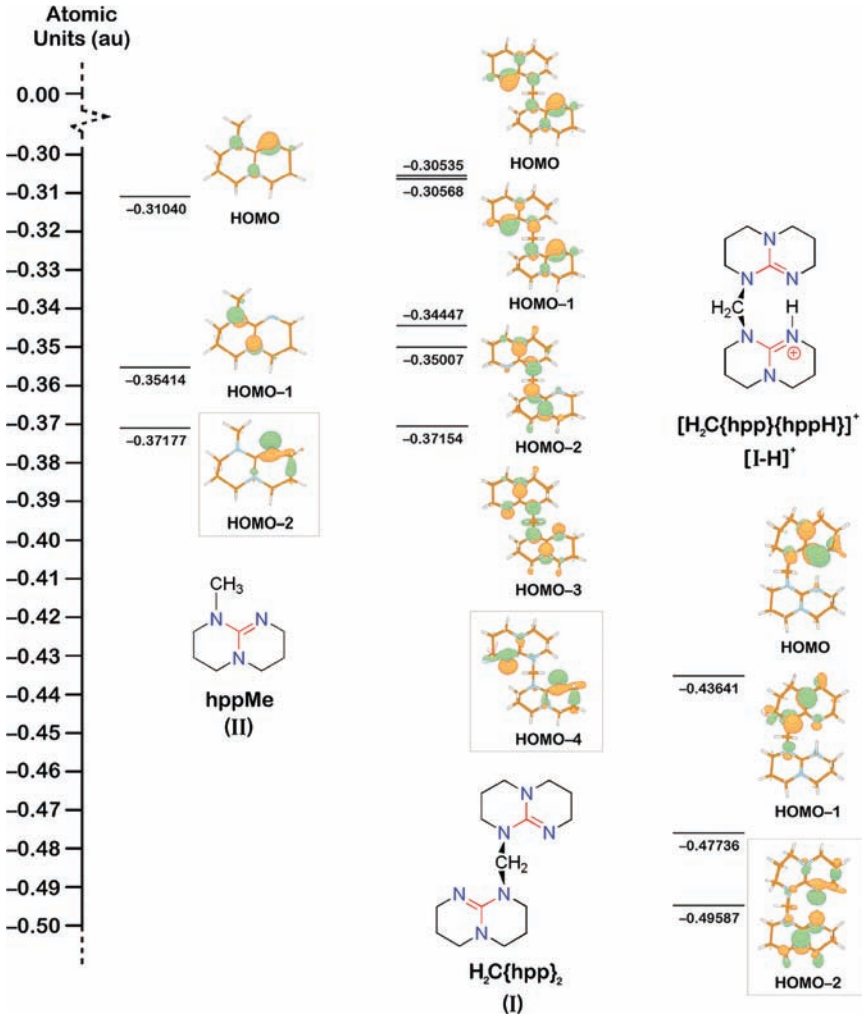

Figure 10. Molecular orbital energy diagram drawn to scale (in atomic units) for hppMe (**II**), $H_2C\{hpp\}_2$ (**I**), and $[H_2C\{hpp\}\{hppH\}]^+$ ($[\mathbf{I}\text{-H}]^+$-*syn*). The boxed orbital represents the PRIMO for each species.

difference in PA for **I** and **II** to be 14.8 kcal mol^{-1} (*vide supra*). To determine which of the three effects dominates, it is useful to define the difference in the PA:

$$\mathrm{PA}(\mathbf{I}) - \mathrm{PA}(\mathbf{II}) = \Delta\mathrm{PA}(\mathbf{I}) = [-\Delta(\mathrm{IE})_n^{\mathrm{Koop}}; \Delta E(\mathrm{ei})_{\mathrm{rex}}; \Delta(\mathrm{BAE})^{\bullet+}] \quad (8)$$

where square brackets imply summation of the three terms within, defined as

$$-\Delta(\mathrm{IE})_n^{\mathrm{Koop}} = -\mathrm{IE}(\mathbf{I})_n^{\mathrm{Koop}} + \mathrm{IE}(\mathbf{II})_n^{\mathrm{Koop}} \quad (9a)$$

$$\Delta E(\mathrm{ei})_{\mathrm{rex}} = E(\mathrm{ei})_{\mathrm{rex}}(\mathbf{I}) - E(\mathrm{ei})_{\mathrm{rex}}(\mathbf{II}) \quad (9b)$$

$$\Delta(\mathrm{BAE})^{\bullet+} = \mathrm{BAE}(\mathbf{I})^{\bullet+} - \mathrm{BAE}(\mathbf{II})^{\bullet+} \quad (9c)$$

Comparing data from Table 3, we obtain

$$\mathrm{PA}(\mathbf{I}) - \mathrm{PA}(\mathbf{II}) = [-0.2; 11.1; 3.9] = 14.8 \text{ kcal mol}^{-1}$$

The predominant influence leading to such a trend in basicity is therefore exerted by the relaxation energy, which mirrors properties of the intermediate stage in the protonation event. Examining the PRIMOs of **I** and **II** (Figure 10), we note that they are HOMO−4 and HOMO−2, respectively, which are of approximately the same energy.

It is interesting to rationalize why it is energetically much less favorable to attach the second proton to **I**, leading to the formation of dication $[\mathbf{I}\text{-H}_2]^{2+}$, than it is for the first protonation (*vide supra*). Triadic analysis offers a simple answer when we consider $[\mathbf{I}\text{-H}]^+$ and $[\mathbf{I}\text{-H}_2]^{2+}$ (Table 3), leading to

$$\mathrm{PA}([\mathbf{I}\text{-H}]^+) - \mathrm{PA}(\mathbf{I}) = [-78.1; -7.9; -7.9] = -93.9 \text{ kcal mol}^{-1}$$

The second protonation is as much as 93.9 kcal mol^{-1} less exothermic than the first, and in this case it is predominantly a consequence of the properties of the initial molecules. This is mirrored through the differences in Koopmans' ionization terms, where in $[\mathbf{I}\text{-H}]^+$ the molecular orbitals are much more stabilized because of an excess positive charge, so that it becomes much more costly to ionize $[\mathbf{I}\text{-H}]^+$ than **I** (Table 3). Still, it is important to note that the overall difference in the basicity of the two molecules is determined by all three terms appearing in the triadic expression, although Koopmans' term is an order of magnitude larger in absolute value than either of the other two contributions.

pK_a Measurement of I by Spectrophotometric Titration. To authenticate the calculations presented above, the acidic dissociation of $[\mathbf{I}\text{-H}]^+$ has been studied in acetonitrile using UV−vis spectrophotometric titrations, enabling the pK_a value

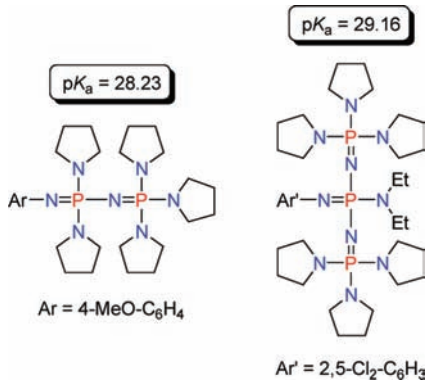

Figure 11. Polyphosphazene reference compounds used to determine the pK_a of [**I**-H]$^+$.

Table 4. Comparison of the Measured Acetonitrile pK_a Values for **I** with Those of Related Amidine and Guanidine Bases

compound	pK_a(obs)	ref
vinamidine proton sponge (**i**)	29.22	12
$H_2C\{hpp\}_2$ (**I**)	28.98	this work
DMAG[a]	27.15	48
hppH	26.03	3
hppMe (**II**)	25.49	3
DBU[b]	24.34	3
PhTMG[c]	20.84	3
DMAN (**a**) proton sponge	18.62	3

[a] *N*,*N*′,*N*″-Tris(3-dimethylaminopropyl)guanidine. [b] Diazabicycloundec-5-ene. [c] Phenyltetramethylguanidine.

for the attachment of the first proton to $H_2C\{hpp\}_2$ (**I**) to be calculated. The experimental procedures for this process have been described in detail in previous publications[47] and are discussed in more detail in the Supporting Information. In the case of [**I**-H]$^+$, measurements were made against two polyphosphazene references of known pK_a (Figure 11).[3] The results show that **I** is a stronger base than 4-MeO-$C_6H_4P_2(pyrr)_5$ by 0.74 ± 0.04 pK_a unit and a weaker base than 2,5-Cl_2-$C_6H_3P_3(pyrr)_6(NEt_2)$ by 0.17 ± 0.02 pK_a unit, with the average for these two results giving pK_a = 28.98 ± 0.05 for [**I**-H]$^+$. This is in excellent agreement with the theoretical estimate of 28.6 units. We note that the experimentally determined pK_a for the paradigmatic proton sponge DMAN (**a**), typically used as a threshold for the classification of a "superbase", is 18.62,[3] emphatically confirming the designation of **I** as a superbase.

Table 4 compares the pK_a of **1b** with the experimentally determined values of related amidine and guanidine bases.[3,48] Results show that $H_2C\{hpp\}$ is a much stronger base than most of the previously studied amidines and guanidines by between approximately 3 (cf. hppH) and 10 (cf. DMEN) orders of magnitude. Only a small selection of neutral organic bases, notably substituted phosphazenes and vinamidine proton sponges, show a greater pK_a under identical experimental procedures.[3]

During the titration experiments for the ΔpK_a determination and after reaching the protonated form of the $H_2C\{hpp\}_2$ (**I**), it was observed from the spectra that when an excess amount of acidic titrant solution is added, [**I**-H]$^+$ binds a second proton to form the dication, $[H_2C\{hppH\}_2]^{2+}$ ([**I**-H_2]$^{2+}$).[20] Measurement of accurate pK_a values involving multiply charged species is, however, complicated due to problems estimating reliable activity coefficients.

Summary and Conclusions

The bis(guanidino) compound, $H_2C\{hpp\}_2$ (**I**), has been converted to the monoprotonated salt $[H_2C\{hpp\}\{hppH\}][X]$ (**1a**, X = Cl; **1b**, X = BPh_4), containing the mixed guanidino/guanidinium cation, [**I**-H]$^+$. Spectroscopic measurements in the solution phase are consistent with a symmetric structure containing an intramolecular hydrogen bond and rapid proton exchange. Although solid-state measurements indicate association of the proton predominantly at one nitrogen, both CPMAS ^{15}N NMR spectroscopy and high-resolution X-ray diffraction show partial protonation of the formally neutral guanidino group, consistent with a solid-state proton-transfer process. The proton affinity and basicity of **I** have been calculated in the gas phase and in MeCN solution, both of which indicate this molecule should be considered as a superbase. This was confirmed by spectrophotometric titrations which gave pK_a = 28.98 ± 0.05 for [**I**-H]$^+$.

The reasons for the high basicity of **I** are two-fold: (i) a high intrinsic basicity of the hpp moiety, as evident by its PA value of 254.6 kcal mol^{-1}, and (ii) the formation of a strong IHB to the second guanidino subunit, which in turn undergoes partial cationic resonance stabilization due to partial protonation. The increase in PA relative to that of hppH is 16 kcal mol^{-1}. Although it has been shown that (poly)alkylation generally increases the basicity of the parent compound both in the gas phase and in solution by enhancing the electron density relaxation effect after protonation,[1,49] the reverse is noted in acetonitrile for the bicyclic guanidine system.[3,50] Hence, the *N*-methylated derivative hppMe less basic than the parent hppH compound, attributed to the more efficient solvation of the $[hppH_2]^+$ cation. The large increase in the basicity of **I** must therefore derive from the presence of the second guanidino functionality and its polarization by the proton linked to the first one. This feature can be characterized as the partial protonation of the second guanidino fragment in a static picture. On the other hand, the dynamic picture is given by fast proton-transfer reaction between equivalent nitrogens N1 and N4, in which the proton is oscillating back and forth between the two positions.

This is corroborated by the solid-state ^{15}N NMR spectroscopy measurements and theoretical studies, which have shown that "hydrogen bond compression" occurs simultaneously as the proton is transferred from one heavy atom to the other in barrierless N···H···N hydrogen bonds,[51] and this has now been observed in a number of systems,[52] including some α-amino acids.[53] We rationalize that the flexibility of the methylene group linking the two guanidino groups in [**I**-H]$^+$ enables the close approach of the two nitrogen atoms, thereby facilitating proton transfer by forming a strong, almost linear HB with no barrier to proton transfer. Indeed, the gas-phase structure of [**I**-H]$^+$-**TS** shows a contraction of 0.19 Å in the N···N distance

(47) (a) Leito, I.; Kaljurand, I.; Koppel, I. A.; Yagupolskii, L. M.; Vlasov, V. M. *J. Org. Chem.* **1998**, *63*, 7868–7874. (b) Kaljurand, I.; Rodima, T.; Leito, I.; Koppel, I. A.; Schwesinger, R. *J. Org. Chem.* **2000**, *65*, 6202–6208. (c) Rodima, T.; Kaljurand, I.; Pihl, A.; Mäemets, V.; Leito, I.; Koppel, I. A. *J. Org. Chem.* **2002**, *67*, 1873–1881.
(48) Eckert-Maksić, M.; Glasovac, Z.; Trošelj, P.; Kütt, A.; Rodima, T.; Koppel, I.; Koppel, I. A. *Eur. J. Org. Chem.* **2008**, 5176–5184.
(49) (a) Maksić, Z. B.; Kovačević, B. *J. Phys. Chem. A* **1998**, *102*, 7324–7328. (b) Maksić, Z. B.; Kovačević, B. *J. Phys. Chem. A* **1999**, *103*, 6678–6684.
(50) Kovačević, B.; Maksić, Z. B. *Org. Lett.* **2001**, *3*, 1523–1526.
(51) Benedict, H.; Limbach, H.-H.; Wehlan, M.; Fehlhammer, W.-P.; Golubev, N. S.; Janoschek, R. *J. Am. Chem. Soc.* **1998**, *120*, 2939–2950.

compared with the ground state. To be more specific, both structures possess N···H···N angles approaching the optimal value of 180° ([**I**-H]$^+$ = 176.9°; [**I**-H]$^+$-**TS** =177.3°), enabling facile proton transfer between nitrogen atoms.

The conformational flexibility and the approximately linear N···H···N angle derive from the structure of the neutral compound and the size of the heterocycle formed by the IHB. This, in turn, stems from the unique position of the bridging atom that links the guanidino groups in **I** (Scheme 1), namely via an amino nitrogen rather than the more usual case in which the N_{imino} atom is a component of the linking group (Figure 1). We also note that most bis-guanidino systems previously developed are based on rigid frameworks which, while they may favorably align the imine nitrogen atoms toward formation of an IHB, restrict any hydrogen bond compression that would facilitate proton transfer. Finally, the formation of an eight-membered heterocycle in [**I**-H]$^+$ is unusual, with most other systems being comprised of either six- (i.e., [DMAN-H]$^+$, [TMGB-H]$^+$, [TMGN-H]$^+$, [DMEGN-H]$^+$, and [TMGBH-H]$^+$) or seven-membered ([TMGBP-H]$^+$ and [TMGF-H]$^+$) rings, which generates more acute N···H···N angles on protonation. Conformational flexibility and linear N···H···N angles, however, do not always lead to simple proton-transfer processes. Recent studies on protonated *N*,*N*,*N*′,*N*′-tetramethylputrescine indicate that the proton is most likely near a potential energy maximum between the two nitrogen atoms, likening the situation to the Buridan's ass paradox.[25] In contrast, the combination of a flexible linker and constituent guanidino groups leads us to conclude that the proton in our system is smarter than Buridan's donkey, with rapid transfer enabling it to take "bites" from both "haystacks", thereby staying alive and kicking.

Acknowledgment. This work was supported by Grants 6699 and 7374 from the Estonian Science Foundation (I.L., I.K.) and by Grant No. 098-0982933-2932 from the Ministry of Science, Education and Sports of the Republic of Croatia (Z.B.M.). R.V. gratefully acknowledges financial support by the Unity through Knowledge Fund (www.ukf.hr) of the Croatian Ministry of Science, Education and Sports (Grant Agreement No. 20/08), together with cofinancing provided by APO Ltd. Environmental Protection Services, Zagreb, Croatia (www.apo.hr). We acknowledge the EPSRC solid-state NMR service at Durham. Generous support of the SRCE Computational Center in Zagreb is thankfully acknowledged.

Supporting Information Available: Full experimental details and details of the X-ray analysis of **1b**; variable-temperature ^{1}H NMR spectra of **1b**; solid-state CPMAS ^{13}C NMR spectrum of **1b**; calculated vs observed bond lengths table for **1b**; details on energies and geometries of all compounds computationally investigated; complete ref 31. This material is available free of charge via the Internet at http://pubs.acs.org.

JA906618G

(52) (a) Aguilar-Parrilla, F.; Scherer, G.; Limbach, H.-H.; Foces-Foces, M. C.; Cano, F. H.; Smith, J. A. S.; Toiron, C.; Elguero, J. *J. Am. Chem. Soc.* **1992**, *114*, 9657–9659. (b) Klein, O.; Bonvehi, M. M.; Aguilar-Parrilla, F.; Elguero, J.; Limbach, H.-H. *Isr. J. Chem.* **1999**, *34*, 291–299. (c) Limbach, H.-H.; Klein, O.; Lopez, J. M.; Elguero, J. *Z. Phys. Chem.* **2004**, *217*, 17–49. (d) Klein, O.; Aguilar-Parrilla, F.; Lopez, J. M.; Jagerovic, N.; Elguero, J.; Limbach, H.-H. *J. Am. Chem. Soc.* **2004**, *126*, 11718–11732. (e) Limbach, H.-H.; Lopez, J. M.; Kohen, A. *Philos. Trans. R. Soc. London, Ser. B* **2006**, *361*, 1399–1415.

(53) (a) Bliznyuk, A. A.; Schaefer, H. F., III; Amster, I. J. *J. Am. Chem. Soc.* **1993**, *115*, 5149–5154. (b) Kovačević, B.; Rožman, M.; Klasinc, L.; Srzić, D.; Maksić, Z. B.; Yanez, M. *J. Phys. Chem. A* **2005**, *109*, 8329–8335.